remote sensing

MDPI

Article

Glacier Changes from 1990 to 2022 in the Aksu River Basin, Western Tien Shan

Pei Ren [1,2,3], Xiaohui Pan [1,2,4,5], Tie Liu [1,2,3,4,5,6,7,*], Yue Huang [1,2,3], Xi Chen [3,4,5,7], Xiaofei Wang [1,2], Ping Chen [8] and Shamshodbek Akmalov [7,9]

1 State Key Laboratory of Desert and Oasis Ecology, Xinjiang Institute of Ecology and Geography, Chinese Academy of Sciences, Urumqi 830011, China; renpei21@mails.ucas.ac.cn (P.R.); panxiaohui@ms.xib.ac.cn (X.P.); huangy@ms.xjb.ac.cn (Y.H.); wangxiaofei201@mails.ucas.ac.cn (X.W.)
2 Key Laboratory of GIS & RS Application, Urumqi 830011, China
3 University of Chinese Academy of Sciences, Beijing 100049, China; chenxi@ms.xjb.ac.cn
4 Sino-Belgian Joint Laboratory of Geo-Information, Urumqi 830011, China
5 Sino-Belgian Joint Laboratory of Geo-Information, 9000 Ghent, Belgium
6 China-Pakistan Joint Research Centre on Earth Sciences, Chinese Academy of Sciences (CAS)-Higher Education Commission (HEC), Islamabad 45320, Pakistan
7 CAS Research Center for Ecology and Environment of Central Asia, Urumqi 830011, China; shamshodbekjon@mail.ru
8 Xinjiang Uygur Autonomous Region Natural Disaster Comprehensive Monitoring and Early Warning Center, Urumqi 830011, China; 2017904402@chd.edu.cn
9 Tashkent Institute of Irrigation and Agricultural Mechanization Engineers (TIIAME), National Research University, Tashkent 999033, Uzbekistan
* Correspondence: liutie@ms.xjb.ac.cn

Abstract: Mountain glaciers are considered natural indicators of warming and a device for climatic change. In addition, it is also a solid reservoir of freshwater resources. Along with climate change, clarifying the dynamic changes of glacier in the Aksu River Basin (ARB) are important for hydrological processes. The study examined the variations in glacier area, elevation, and their reaction to climate change in the ARB between 1990 and 2022. The glacier melt on the runoff is explored from 2003 to 2020. This investigation utilized Landsat and Sentinal-2 images, ICESat, CryoSat, meteorological and hydrological data. The findings suggest that: (1) The glacier area in the ARB retreated by 309.40 km^2 (9.37%, 0.29%$\cdot$a^{-1}) from 1990 to 2022. From 2003 to 2021, the ARB glacier surface elevation retreat rate of 0.38 $\pm$ 0.12 m$\cdot$a^{-1} (0.32 $\pm$ 0.10 m w.e.a^{-1}). Comparison with 2003–2009, the retreat rate is faster from 2010 to 2021. (2) From 1990 to 2022, the Toxkan and the Kumalak River Basin's glacier area decreases between 61.28 km^2 (0.28%$\cdot$a^{-1}) and 248.13 km^2 (0.30%$\cdot$a^{-1}). Additionally, the rate of glacier surface elevation declined by -0.34 ± 0.11 m$\cdot$a^{-1}, -0.42 ± 0.14 m$\cdot$a^{-1} from 2003 to 2021. (3) The mass balance sensitivities to cold season precipitation and ablation-phase accumulated temperatures are +0.27 $\pm$ 0.08 m w.e.a^{-1}(10%)$^{-1}$ and -0.33 ± 0.10 m w.e.a^{-1} °C^{-1}, respectively. The mass loss is (962.55 $\pm$ 0.57) $\times$ 10^6 m^3 w.e.a^{-1}, (1087.50 $\pm$ 0.68) $\times$ 10^6 m^3 w.e.a^{-1} during 2003–2009, 2010–2021 respectively. Warmer ablation-phase accumulated temperatures dominate glacier retreat in the ARB. (4) Glacier meltwater accounted for 34.57% and 41.56% of the Aksu River's runoff during the ablation-phase of 2003–2009 and 2010–2020, respectively. The research has important implications for maintaining the stability of water resource systems based on glacier meltwater.

Keywords: climate change; glacial variations; water resources; the Aksu River Basin

check for updates

Citation: Ren, P.; Pan, X.; Liu, T.; Huang, Y.; Chen, X.; Wang, X.; Chen, P.; Akmalov, S. Glacier Changes from 1990 to 2022 in the Aksu River Basin, Western Tien Shan. *Remote Sens.* **2024**, *16*, 1751. https://doi.org/10.3390/rs16101751

Academic Editors: Ulrich Kamp, Dmitry Ganyushkin and Bijeesh K. Veettil

Received: 7 April 2024
Revised: 19 April 2024
Accepted: 19 April 2024
Published: 15 May 2024

1. Introduction

The regulation of river runoff downstream is significantly influenced by the snow and glacier meltwater. The Tien Shan region, known for its high concentration of mountain glaciers, boasts a staggering 10,778 glaciers covering a combined area of 13,566.60 km^2.

Under global warming, 97.25% of glaciers in the Tien Shan have shown retreat in the past 50 years [1]. The glacier area change rate was $-0.11\%\cdot a^{-1}$ in 1975–2008 [2], and the glacier volume has decreased by about 27 ± 15% in the last 50 years [3]. At the same time, the frequency of sudden disasters has significantly increased, such as avalanches, glacial lake outburst floods, and glacier mudslides [4–7]. Seriously affecting the downstream production and ecological environment.

Climate change causes the redistribution of water resources in spatiotemporal and changes in total water resources. Glaciers in the ARB are in a state of retreat. He [8] found that the area of Tomur Peak glacier decreased by 264 km^2 (11.78%) from 1990 to 2011, and the annual percentage of area changes (APAC) was $0.54\%\cdot a^{-1}$. Zhang [9] explored the glacier changes in the ARB from 1975 to 2016, the results showed that the glacier area, and volume retreated 965.7 km^2 (25.88%), 74.85 km^3 (23.72%). Glacier mass loss can be more accurately estimated using glacier elevation change. Currently, glacier surface elevation changes are mainly monitored by satellite gravity, geodesy and satellite altimetry. The satellite gravity method has a low spatial resolution, which makes it difficult to be used for small-scale glacier mass balance. The geodetic method makes it difficult to monitor the glacier surface elevation changes accurately and continuously because of the large difference in the years of multi-source DEM data and the error in the alignment process. Satellite altimetry has high precision and wide coverage and can continuously acquire glacier surface elevation changes. Pieczonka [10] explored the change of glacier surface elevation in the Aksu-Tarim Basin of -0.33 ± 0.15 $m\cdot a^{-1}$ during 1976–2009 using KH-9 Hexagon and SPOT-5 stereo image data. Burn [11] explored the mass balance change of Tianshan glacier using digital elevation model time series obtained from satellite stereo imagery and showed that the rate of change of material balance from 2000–2016 was -0.28 ± 0.20 m w.e.a^{-1}. Wang [12] combined with ICESat-1&2 and GRACE data, provided a continuous glacier elevation surface change of -0.45 ± 0.10 $m\cdot a^{-1}$ for Tien Shan from 2003–2019. However, most previous research works focused on the area before 2011, and there have been few studies on the spatiotemporal changes of glacier area and elevation in the ARB over the last 20 years. Furthermore, a thorough examination of the influence of climate change on glaciers in the ARB is imperative, along with evaluating the contribution of glacial meltwater to runoff. An accurate assessment of recent glacier fluctuations in the ARB is great significance for oasis development and sustainable water resource utilization.

Therefore, this study aims to investigate the changes in glaciers in the ARB from 1990 to 2022 using multi-sources remote sensing data, Randolph Glacier Inventory (RGI 6.0), SRTM DEM, ICESat, CryoSat, meteorological and hydrological data. Band ratio threshold is utilized to extract glacier area. Using the pseudo-repeat track method, the extraction of glacier elevation changes in the ARB from 2003 to 2021. The effects of major meteorological factors on glacier retreat and the contribution of glacier melt to runoff are explored, respectively. The results can support the improvement of disaster prevention and mitigation benefits, as well as the development of climate change adaptation strategies.

2. Materials and Methods

2.1. Study Area

The Aksu River originates from Kyrgyzstan and has two mainstreams, the Kumalak River and the Toxkan River (Figure 1). The Toxkan River is 457 km long. The glaciers in the Toxkan River Basin (TRB) cover 3.66% of the basin area, with the average area of a single glacier being 0.69 km^2 [13]. The length of the Kumalak River is 3730 m. The Kumalak River Basin (KRB) has developed a large area of glacial and snow, with a glacier cover of 16.34% and an average area of 1.36 km^2 for a single glacier. Two tributaries, the Toxkan and Kumalak rivers, converge in Aksu-Karaduvi and join the Tarim River from north to south [14].

The ARB is inland, typical for a temperate continental climate with obvious seasonal variation. The ARB receives most of its water vapor from the Atlantic airflow. The precipitation in the middle and high mountains above 4000 m [15]. The average annual temperature of the mountainous areas and the plains oasis are at 8 °C and 10 °C, respectively [9].

The Aksu River is a typical river that primarily receives water from the melting of snow and glaciers, constituting over half of the river's total runoff [16]. Aksu River runoff is mainly concentrated in the summer, and the summer runoff of June and August accounted for about 65% of the total annual runoff.

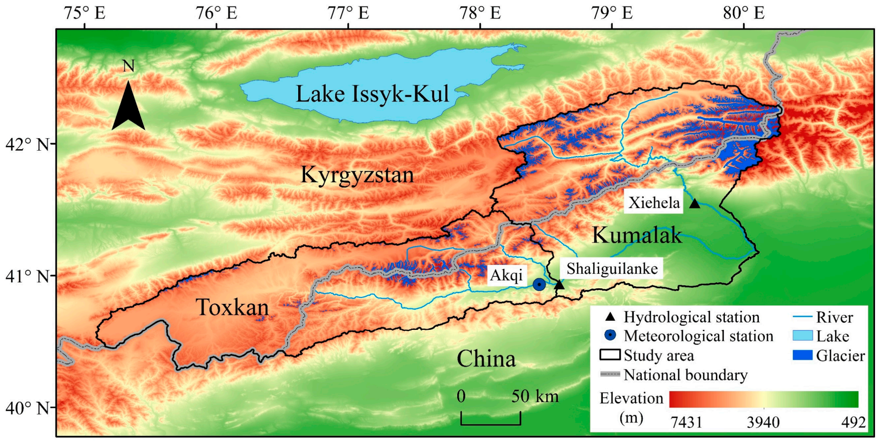

Figure 1. Location of the study area.

2.2. Data Collection

The Landsat TM/ETM+ images in 1990, 2000, 2010, and the Sentinal-2 images in 2022 were selected as the data sources for the glacier boundary extraction in the ARB. To minimize the effect of seasonal snow and clouds on potential uncertainties in determining glacier boundaries, we selected reference scenes with minimal or no cloudiness during the glacier ablation period (June–September). Due to the absence of image data or low image quality in individual areas during the study period, images forward-shifted 1–3 years were used instead (Table 1). The glacier inventory data derived from RGI 6.0 was referenced during glacier boundary extraction.

Table 1. List of the remote sensing images used.

Year	Data	Path/Row	Sensor	Spatial Resolution
1990	22 August 1989 19 August 1991 25 September 1993 20 September 1990 7 August 1990 7 August 1990	147/31 148/31 148/31 148/32 149/31 149/32	Landsat TM	30 m
2000	26 August 1999 26 August 1999 22 August 1998 23 August 1996 29 August 1998	147/31 148/31 148/32 149/31 149/32	Landsat ETM+ Landsat TM	30 m
2010	3 August 2011 11 September 2011 11 September 2011 27 August 2009 16 July 2011	147/31 148/31 148/32 149/31 149/32	Landsat TM	30 m
2022	26 July 2022 26 July 2022 26 July 2022 26 July 2022 27 September 2022 27 September 2022	T44TKL T44TKM T44TLM T44TMM T43TEF T43TFF	Sentinel MSI	20 m

The SRTM DEM was selected to provide auxiliary information for screening outliers and initial values for estimating glacier elevation change in the ARB. The SRTM C band signals penetrate snow and glaciers, and differences in glacier surfaces lead to large variations in the depth of penetration in different regions. The penetration depth of SRTM C band DEM in different glacial regions over the High Mountain Asia (HMA) was calculated and compared with the SRTM X band DEM [17]. The result showed that this study area's SRTM C-band penetration depth is 1.8 m.

ICESat/GLAS 14 products covering glaciers in the ARB from 2003 to 2009 were selected to analyze the glaciers' surface elevation change in the ARB. As a radar altimetry satellite, the CryoSat-2 data are dense and 5–6 times more intensive than the ICESat data [18]. This study selected CryoSat-2 SARIn L2I satellite altimetry data during the non-ablation period to estimate the variation in glacier elevation between 2010 and 2021.

Akqi Meteorological Station is located in the central region of the ARB at an elevation of 1986 m. Monthly precipitation and temperature from 1957 to 2022 have been collected at the Akqi Meteorological Station. Due to there being only one meteorological station in the study area, it is impossible to indicate the climate characteristics. We selected the precipitation from the Global Precipitation Climate Center (GPCC) from 1990 to 2020. The spatial resolution of GPCC is 0.25°, and the application performs better in mountainous areas with complex topography [13]. The ERA5-Land reanalysis data contains 50 climate variables covering all land areas of the globe with a spatial resolution of 0.1°, and is widely used in research areas where long-term climate change observations are lacking [19]. The 2 m air temperature from 1990 to 2022 is selected for this study. Since the GPCC precipitation ends in 2020, the ERA5-Land precipitation data from 2021 to 2022 is selected to be resampled to 0.25°, it can be obtained from 1990–2022 with a resolution of 0.25° precipitation.

The 2003–2020 runoff data in the ARB were obtained from the sum of runoff from Shaliguilanke and Xiehela hydrological stations. The runoff was obtained from the observations of the hydrological stations in their respective headwater areas and were all provided by the Xinjiang Uygur Autonomous Region Hydrological Bureau.

2.3. Methods

In this paper, glacier area is extracted for 1990, 2000, 2010 and 2022 based on Landsat and Sentinal-2 images based on band ratio threshold. Glacier elevation changes in the ARB from 2003–2021 are calculated based on ICESat, CryoSat, and SRTM using the pseudo-repeat track method. Considering the glacier area and surface elevation changes, the amount of glacier material (volume) change was calculated (Figure 2).

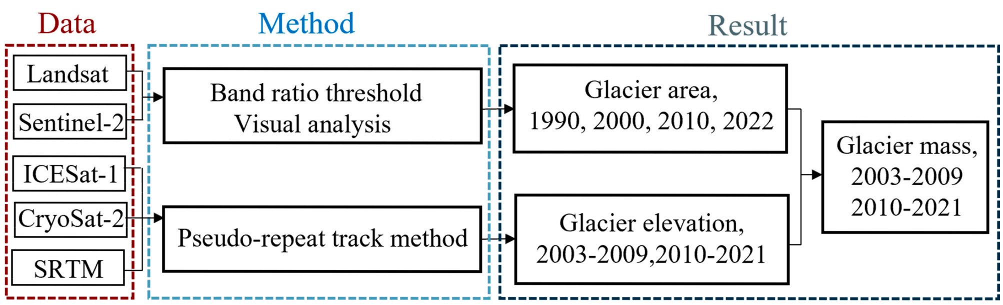

Figure 2. Main technical route.

2.3.1. Glacier Mapping

Glacier outlines were extracted based on Landsat and Sentinel-2 using the band ratio threshold. This method has been extensively employed in the extraction of glacier areas, with an error of about 3% to 5% [20–22]. The most accurate glacier boundaries were extracted at a threshold of 2.0 as determined by empirical thresholding in conjunction with visual interpretation of remote sensing images. The false-color image and digital elevation were used as the base map, and the glacier boundary was carefully corrected by manual digitization. The Automatic extraction method of Satellite imagery struggled to map moraine and debris-covered glaciers accurately. Thus, we delineate the glacier boundary mainly through visual analysis of some surface features, such as the glacier surface moraine, ice surface lakes, and the water system at the end of the glacier.

We utilized a minimum glacier area of 0.01 km^2 [23] to classify glaciers in the ARB into the following 10 classes: 0.01–0.1 km^2; 0.1–0.5 km^2; 0.5–1 km^2; 1–2 km^2; 2–5 km^2; 5–10 km^2; 10–20 km^2; 20–30 km^2; 30–50 km^2; >50 km^2, and analyze the changes of glacier number and area at each scale.

2.3.2. Pseudo-Repeat Track Method

The glacier elevation is a significant factor in glacier mass variation and a key parameter for analyzing glacier changes under climate change. The pseudo-repeat track method treats a grid as a plane and uses all transit altimeter data within a grid to perform plane fitting. Then, the glacier elevation change rate is calculated based on the relevant fitting parameters [24–27]. The advantage of the algorithm is that it can fully utilize the transit altimeter point. At the same time, it can comprehensively consider the influence of surface topography within a grid by introducing DEM data [28].

To obtain accurate glacier elevation changes, it is necessary to select transit tracks and valid altimeter points falling within the glacier area. First, anomalous data are rejected by multiple quality labeling of ICESat/GLA14, CryoSat-2 altimetry points. Second, CryoSat-2 data coarseness was rejected using statistical methods (3-fold median error, Shoveler, first-order difference). Third, the 30 m resolution SRTM data are used as the benchmark data to remove anomalies of ICESat and CryoSat-2 altimetry data at corresponding geographic locations through the thresholding method (with the threshold value of 100 m). Obtaining the altimetry data with no anomalies on the glacier to calculate the glacier surface elevation rate.

2.3.3. Uncertainty Assessment

The accuracy of glacier area extraction is affected by several factors [29,30]. In this paper, errors due to image quality can be greatly ameliorated by selecting images at the ablation period, as well as images from neighboring years. Errors in glacier outline extraction due to sensor differences and image alignment errors were evaluated using an uncertainty formula [29]:

$$\alpha = 2\lambda\sqrt{\lambda^2 + \varepsilon^2} \tag{1}$$

where α is the uncertainty in the glacier area extraction, λ and ε are the imagery spatial resolution and alignment error. The errors in calculating the area of individual glaciers by Landsat and Sentinel-2 were ± 0.0025 km^2, ± 0.0003 km^2. In this study, the uncertainty of glacier area was calculated to be ± 6.43 km^2, ± 6.32 km^2, ± 6.21 km^2 and ± 0.73 km^2 for 1990, 2000, 2010, and 2021, which accounted for 0.19%, 0.20%, 0.20% and 0.02% of the glacier area, respectively.

The accuracy of calculating glacier surface elevation changes using the pseudo-repeat track method is as follows:

$$Q_{\hat{x}\hat{x}} = \left(B^T PB\right)^{-1} = \begin{bmatrix} Q^2_{\alpha_E} & Q_{\alpha_E,\alpha_N} & Q_{\alpha_E,ht} \\ Q_{\alpha_E,\alpha_N} & Q^2_{\alpha_N} & Q_{\alpha_N,ht} \\ Q_{\alpha_E,ht} & Q_{\alpha_N,ht} & Q^2_{ht} \end{bmatrix} \tag{2}$$

$$\sigma_0 = \sqrt{V^T PV/(n-t)} \tag{3}$$

$$\sigma_{ht} = \sigma_0 Q_{ht} \tag{4}$$

where $Q_{\hat{x}\hat{x}}$ represents the covariance matrix of parameter estimation while Q_{α_E}, Q_{α_N}, and Q_{ht} are the autocovariance matrices of α_E, α_N, and dh/dt, respectively. B is the coefficient matrix of the error equation, V is the observation correction matrix, σ_0 and n are the unit weight standard deviation and the number of observed points within the observation plane, t is 3 in this paper. σ_{ht} represents the error associated with elevation changes.

3. Results

3.1. Glacier Area Changes in the ARB

There are 2430 glaciers in the ARB in 2022 with an area of 2992.56 ± 0.73 km^2, which is 7.06% of the basin area. From 1990 to 2022, the glaciers in the ARB were in retreat with a loss of 309.40 km^2 (9.37%), and an APAC was −0.29%·a^{-1}. The APAC is similarly around −0.30% at different times (Table 2).

Table 2. Glacier area retreat in the ARB.

Year	Number	Area (km^2)	Variation (km^2)	Variation Percentage (%)	APAC (%·a^{-1})
1990	2571	3301.96 ± 6.43	-	-	-
2000	2527	3208.51 ± 6.32	−93.45	−2.83	−0.28
2010	2485	3107.13 ± 6.21	−101.39	−3.16	−0.32
2022	2430	2992.56 ± 0.73	−114.57	−3.69	−0.31
Total	−141	-	−309.40	−9.37	−0.29

Most of the glaciers in the ARB are relatively small to medium in size (Figure 3). According to the data presented in Table 3, the number and area of glaciers with glacier size ≥0.1 km^2 show a decreasing trend from 1990 to 2022. Due to the melting glaciers, the number of glaciers with an area less than 0.1 km^2 and 20–30 km^2 increased by 145 (78%) and 3 (68%), respectively. Glacier areas with 1–2 km^2 are the most prominent trend of retreat, with the number and area of glaciers decreasing by 27% and 20%, respectively. Compared with small and medium-sized glaciers, larger glaciers have more stable changes and slower retreat rates.

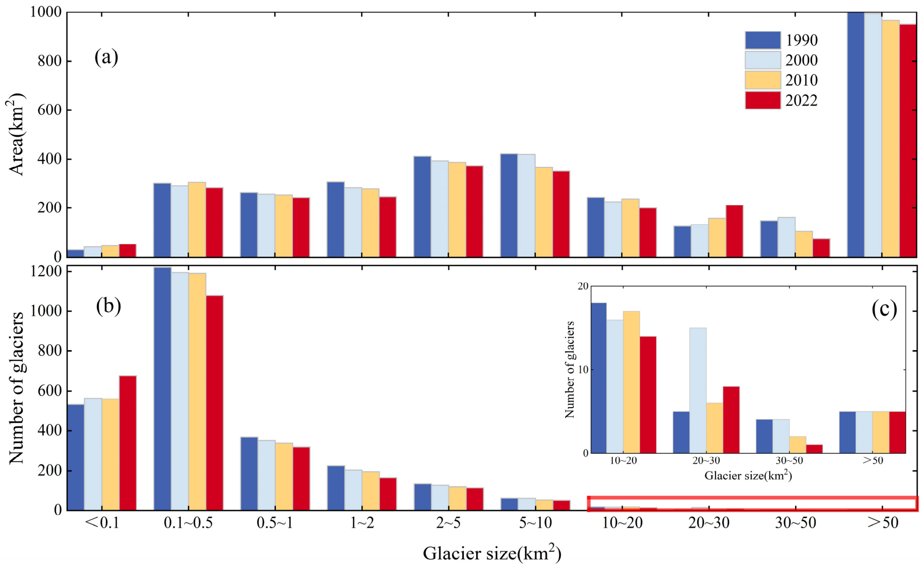

Figure 3. Changes in number (**a**) and area (**b**) of glaciers in the ARB from 1990 to 2022; (**c**) glacier number changes of glacier size >10 km^2.

Most of the glaciers are concentrated at elevations ranging from 3500 to 5000 m (Figure 4a), such as approximately 80.72% of the overall glacier area in 2022. Glacier area is decreasing at all elevations (Figure 4b) except at 2500–3000 m. The absolute area loss of glacier is the largest in the 3000–5000 m due to the higher concentration of glaciers at this altitude.

Table 3. Glacier changes for various glacier size from 1990 to 2022.

Glacier Size (km^2)	<0.1	0.1–0.5	0.5–1	1–2	2–5	5–10	10–20	20–30	30–50	>50
Number change	145	−141	−51	−61	−20	−11	−4	3	−2	0
Number change (%)	27	−12	−14	−27	−15	−18	−22	60	−75	0
Area change (%)	78	−7	−8	−20	−9	−17	−18	68	−14	−9

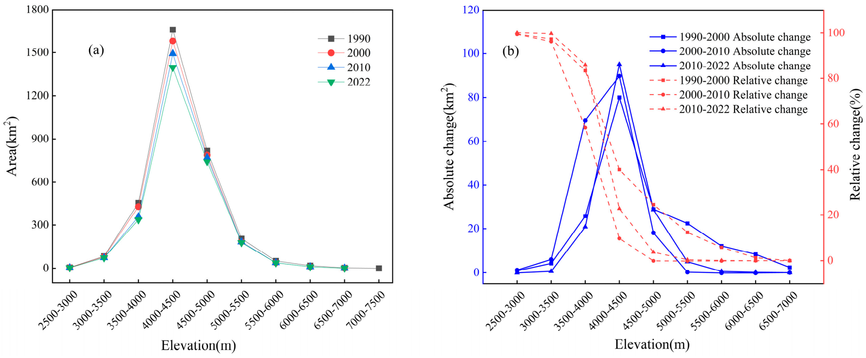

Figure 4. Changes in glacier distribution (**a**) and area (**b**) at different altitudes from 1990 to 2022.

The distribution of glaciers in mountainous areas is not only related to altitude, but also to orientation. Figure 5a shows the distribution of glaciers within the ARB, which shows obvious asymmetry. Glaciers are mainly distributed in the north and northwest directions, accounting for 40.99% of the total glacier area. Northerly (N, NW, and NE) and southerly (SE, S, and SW) glacier areas account for 54.28% and 29.81% of the total glacier area, respectively. More precipitation occurs in the northern region due to the westward wind and the moist flow originating from the Arctic Ocean [31]. The northern region has less solar radiation, thus making it more favorable for glacier development [19]. Figure 5b shows that the glacier area in all directions is in retreat from 1990–2022. The glacier retreat in the last 30 years appears to have shifted from the north to the southeast.

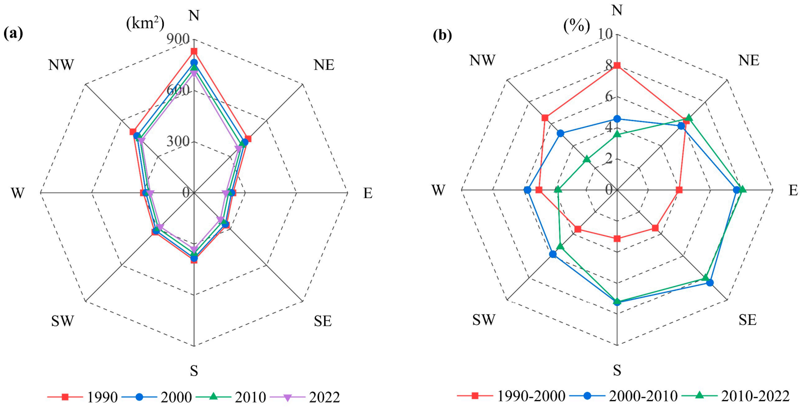

Figure 5. The distribution (**a**) and variations (**b**) of glacier area on different orientations during 1990–2022.

3.2. Glacier Elevation Changes in the ARB

The elevation changes of each altimetry footpoint from 2003 to 2009 and 2010 to 2021 were obtained based on ICESat/GLA and CryoSat-2 altimetry data using the pseudo-repeat track method, respectively. To convert elevation change to mass change, we select a conversion factor of 850 kg·m^{-3} by Huss [32].

The glacier elevation in the ARB from 2003 to 2009 was generally in an ablation state (Figure 6). The glacier elevation change rate was −0.35 ± 0.11 m·a^{-1} (−0.30 ± 0.09 m w.e.a^{-1}), mass loss is (962.55 ± 0.57) × 10^6 m^3 w.e.a^{-1}, equivalent to 0.96 Gt of water.

Compared to the large glaciers within the Tomur Peak, small and medium-sized glaciers in the central part of the ARB have a greater rate of elevation change.

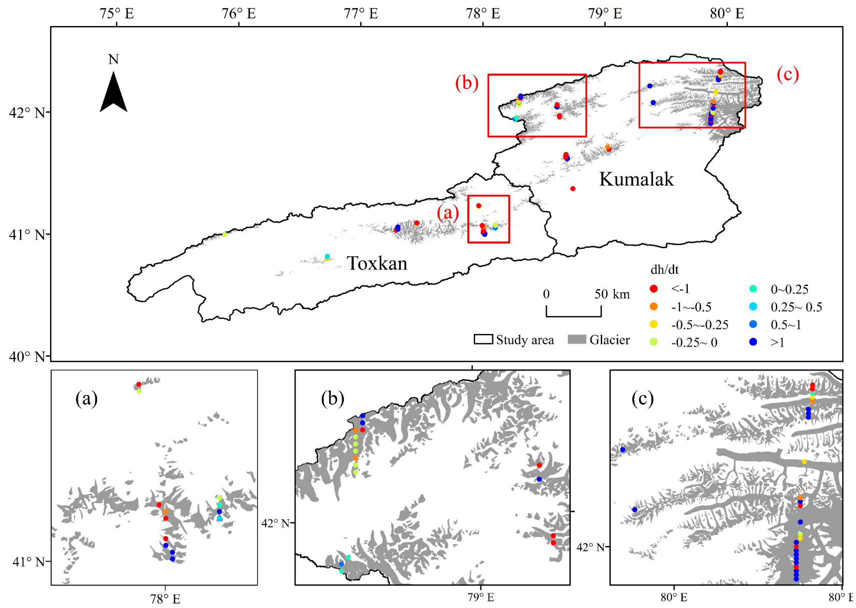

Figure 6. The rate of change in glacier surface elevation from 2003 to 2009 in the central (**a**), the northern (**b**), and the northeastern (**c**) of the basin.

The analysis of glacier surface elevation change between 2010 and 2021 reveals that the glaciers within the ARB are in a negative mass balance (Figure 7). The rate of glacier surface elevation decline is -0.41 ± 0.13 m·a^{-1} (-0.35 ± 0.11 m w.e.a^{-1}), the mass loss is $(1087.50 \pm 0.68) \times 10^6$ m^3 w.e.a^{-1} during 2010 to 2021, which is equivalent to 1.09 Gt of water. Compared with 2003–2009, the rate of glacier elevation change decline increased by 17.14% in 2010–2021. The proportion of glacier elevation melting in the altimetry points increased from 50.70% to 67.97%. The results show that the glacier elevation in the ARB was in a state of ablation from 2003 to 2021, and the rate of glacier volume gradually accelerated.

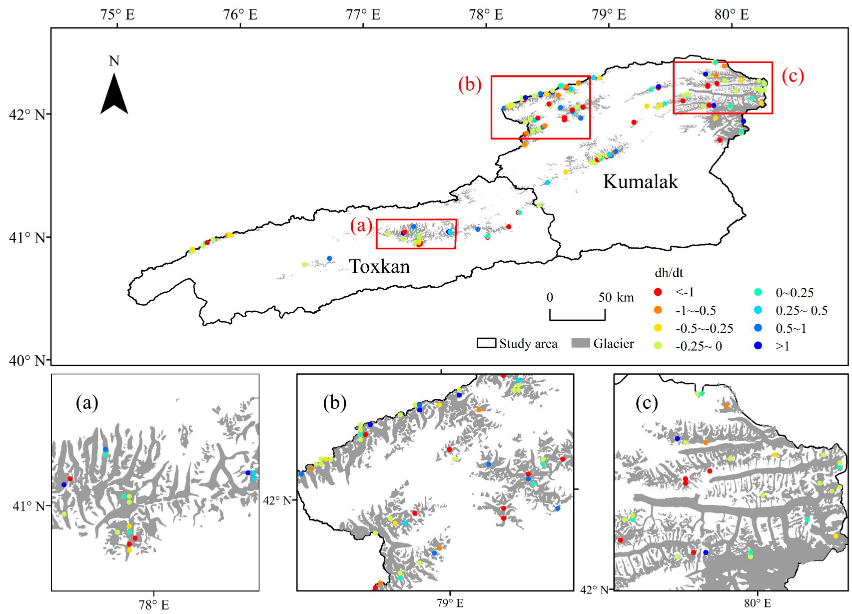

Figure 7. The rate of change in glacier surface elevation from 2010 to 2021 in the central (**a**), the northern (**b**), and the northeastern (**c**) of the basin.

3.3. Glacier Changes in Sub-Basin Scales

There are significant differences in glacier distribution between the TRB and KRB (Table 4, Figure 8). The number of glaciers in the TRB and KRB decreases by 51 (5.93%), 150 (8.77%), and the basin's glacier coverage decreases by 0.31% and 1.09%, respectively. The KRB experienced the most significant decline in glacier numbers during 1990–2000, with a decrease of 2.92%. The number of TRB glaciers increased by 6 from 1990 to 2000 (0.70%), which should be related to the ablation of glaciers into multiple smaller glaciers.

Table 4. Glacier retreat in sub-basin from 1990 to 2022 in the sub-basin.

Sub-Basin	Glacier Number				Glacier Area Proportion (%)			
	1990	2000	2010	2022	1990	2000	2010	2022
TRB	860	866	849	809	3.42	3.39	3.18	3.11
KRB	1711	1661	1636	1621	11.51	11.13	10.86	10.42

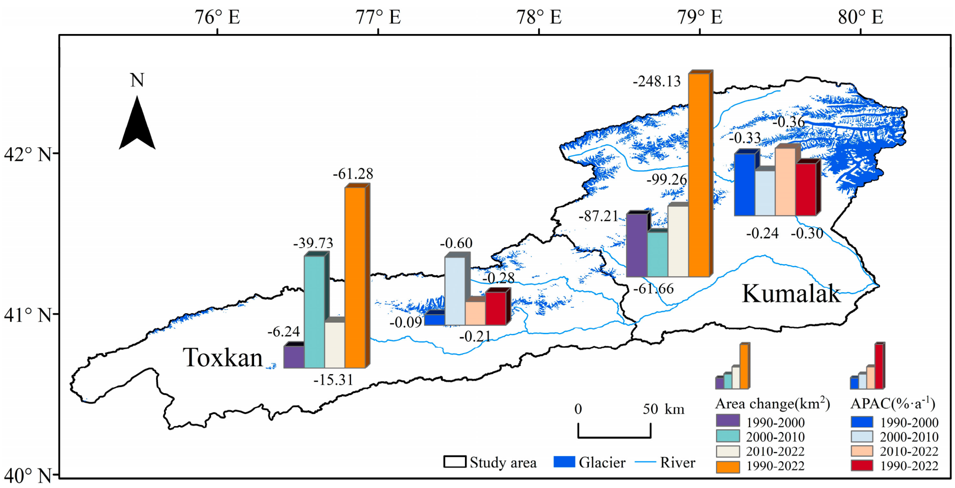

Figure 8. Change in glacier area within the sub-basin between 1990 and 2022.

The TRB glacier area decreased by 61.28 km^2 from 1990 to 2022, with an APAC of $-0.28\%\cdot a^{-1}$. Glacier area retreat was the most drastic in 2000–2010, with an APAC of $-0.60\%\cdot a^{-1}$. The glacier area in the KRB decreased by 248.13 km^2, with an APAC of $-0.30\%\cdot a^{-1}$. Except for 2000–2010, the retreat rate of the KRB glacier area has been more intense than that of the TRB over the last 30 years.

Spatial differentiation in glacier elevation change and mass balance change in the ARB is clearly evident according to Table 5. Glacier surface elevation decline rates in the TRB in 2003–2009 and 2010–2021 were 0.32 ± 0.10 m$\cdot$a^{-1} and 0.36 ± 0.11 m$\cdot$a^{-1}, respectively. In the KRB, the speed of glacier surface elevation alteration is higher, with surface elevation change rate of -0.46 ± 0.15 m$\cdot$a^{-1} between 2010 and 2021. Compared to 2003–2009, the recent TRB and KRB glacier surface elevation retreat rates in 2010–2021 increased by 12.50% and 21.05%.

Table 5. Change in glacier elevation and mass balance in the sub-basin.

Sub-Basin	Changes in Glacier Elevation (m$\cdot$a^{-1})		Changes in Mass Balance (m w.e.a^{-1})	
	2003–2009	2010–2021	2003–2009	2010–2021
TRB	-0.32 ± 0.10	-0.36 ± 0.11	-0.27 ± 0.09	-0.31 ± 0.09
KRB	-0.38 ± 0.12	-0.46 ± 0.15	-0.32 ± 0.10	-0.39 ± 0.13

3.4. Changes in the Typical Glacier

The Tien Shan's largest region of contemporary glacial activity is Tomur Peak [33–35], which serves as the primary origin of the Tarim River [36]. Tianshan Glaciological Station, Chinese Academy of Sciences organized a field trip working group to have a more systematic understanding of the area, thickness and, moraine of the Qingbingtan Glacier No. 72 in the Tomur Peak over the past 60 years [36–38]. This paper focuses on Qingbingtan Glacier No. 72 is selected as a typical glacier in the ARB, hereinafter referred to as Glacier No. 72. With glacier ID RGI60-13.43165, Glacier No. 72 has an area of 5.61 km^2 and a length of 7.4 km. The glacier is mainly recharged by precipitation and avalanches [39].

The Glacier No. 72 area is retreating (Table 6), and the retreat amount is 0.94 km^2 (13.51%), with an average annual decrease of 0.03 km^2. Wang et al. [36] used RTK-GPS and topographic maps to analyze glacier area variation. The results indicated that the Glacier No. 72 area decreased by 0.03 km^2·a^{-1}, which aligns with the findings of this study. Using Cryosat-2 to analyze the glacier surface elevation retreat rate of Glacier No. 72 from 2010 to 2022 was -0.43 ± 0.07 m·a^{-1} (-0.37 ± 0.06 m w.e.a^{-1}). Che et al. [39] analyzed mass balance variations of Glacier No. 72 from 2008 to 2014. The result showed that the mass balance was -0.38 m w.e.a^{-1}, a value that falls within a 5% range of the outcomes obtained in this study. Figure 9 shows that the glacier area retreat of Glacier No. 72 from 1990 to 2021 is significant decline in the glacier tongue. The faster the change of glacier elevation is near the end of the tongue.

Table 6. Glacier area retreat in the typical glacier.

Year	Area (km^2)	Variation (km^2)	Variation Percentage (%)	APAC (%·a^{-1})
1990	6.96	-	-	-
2000	6.71	−0.25	−3.59	−0.36
2010	6.60	−0.11	−1.64	−0.16
2022	6.02	−0.58	−8.79	−0.73
Total	-	−0.94	−13.51	−0.44

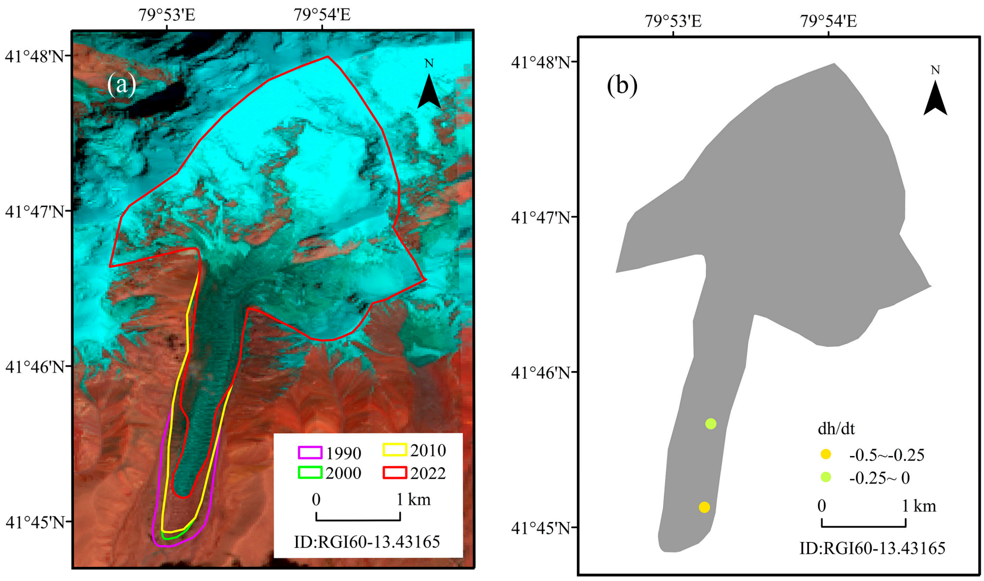

Figure 9. Changes in typical glacier. (**a**) Glacier outlines extracted from remote sensing images; (**b**) annual change rate of glacier elevation from 2010 to 2021.

4. Discussion

4.1. Uncertainty

The glacier results extracted by remote sensing images will be affected by many factors such as data and methods. First, to prevent the impact of seasonal snow and clouds, the glacier boundary is extracted by selecting the image of the glacier ablation period with very little or no clouds. Due to the location of the tongue of some glaciers in the ARB are covered with surface moraine and debris, the band ratio threshold can't accurately extract the region. In this paper, the boundaries of the glacier were visually determined according to the characteristics of the glacier ends. The area extraction error was evaluated, and the results suggested that the errors in 1990, 2000, 2010, and 2022 were less than 1%. Therefore, it is considered that the glacier boundary extracted in this paper is within the acceptable range and accurate, which is suitable for practical applications. However, since this paper adopts two kinds of remote sensing images for glacier area extraction, the cross-application problem between multi-source data should be considered in the follow-up work.

Qingbingtan Glacier No. 72 is a composite valley glacier. The shape is irregular, movement speed is faster, and the ice tongue accounts for the total length of the ratio, which is significant. The rate of glacier area change of No. 72 glacier has fluctuated greatly in the past 30 years, which is different from that of ARB and sub-basins. To explore the drastic changes of APAC of Glacier 72, it is necessary to consider many influencing factors, such as glacier movement speed, temperature, etc., which need to be further researched and discussed in the future.

ICESat and CryoSat-2 products were utilized to explore the glacier elevation changes in the ARB. For CryoSat-2 data, outliers should be removed not only by quality labeling and statistical methods but also by combining them with DEM data, as well as from the altimeter waveform optimization classification to select the most effective observations in the study area. The use of multi-source satellite altimetry data can explore the changes of glacier elevation in a continuous long time series. Considering that the accuracy and data processing method of each satellite data are different, the processing method of multi-source altimetry data fusion will be a part of the next step.

4.2. Glacier Change in the ARB

The area of Tien Shan glaciers is in a state of retreat, with an area change rate of -18.41% from 1959 to 2010 [40]. The glacier retreat was more intense in the Western Tien Shan. Chen's results showed that the Western Tien Shan glacier area retreat was faster in 2000–2012 compared to the 1960s–2000, with an APCA of $-0.68\%\cdot a^{-1}$ [1]. We find the glacier area retreat rate of the ARB, TRB, and KRB was $0.29\%\cdot a^{-1}$, $0.28\%\cdot a^{-1}$, and $0.30\%\cdot a^{-1}$ during 1990–2022, respectively. Our estimation of glacier area retreat is slightly higher than that of Zhang's result [9]. This is consistent with Oerleman's prediction that glaciers in the 21st century will retreat faster due to global warming [41]. Compared with the TRB, the glacier area change in the KRB has been more drastic in the last 30 years. This finding aligns with the outcome of Zhang [9]. There are fewer studies on glacier surface elevation changes. The Tien Shan glacier surface elevation is melting in the last 20 years [11,12]. The glacier surface elevation retreat rate calculated in our study is $0.38 \pm 0.12\ m\cdot a^{-1}$ during 2003–2021. The result is similar to that of Pieczonka and Bolch [2], which is consistent with the trend of surface elevation variation in the Tien Shan glacier (Table 7).

Accompanied by the wide application of remote sensing satellite data in glacier monitoring, a large number of studies have been conducted on glacier changes. The results show that most glaciers are retreating, but the degree of retreat varies widely (Table 8). Compared with other western mountain systems, the ARB has seen less glacier area retreat and greater changes in glacier surface elevation, which should be monitored more closely. Meanwhile, glacier retreat in the region may have a series of negative impacts on downstream water management and ecosystems, which deserve focused attention.

Table 7. Statistics on glacier changes in previous studies.

Region	Period	Area Variation Percentage (%)	APAC (%·a^{-1})	Elevation Change Rates (m·a^{-1})	Source
Tien Shan	1959–2010	−18.41	−0.36	-	[40]
	2003–2019	-	-	−0.45 ± 0.10	[12]
	2000–2016	-	-	−0.33 ± 0.24	[11]
Western Tien Shan	1960s–2000	−20.00	-	-	[1]
	2000–2012	−8.10	−0.68	-	
ARB	1975–2016	−25.88	−0.63	-	[9]
	1990–2016	−6.50	−0.25	-	[9]
	1975–1999	-	-	−0.35 ± 0.34	[2]
	1990–2022	−9.37	−0.29		This study
	2003–2021	-	-	−0.38 ± 0.12	
TRB	1990–2016	−6.76	−0.26	-	[9]
	1990–2022	−8.96	−0.28		This study
	2003–2021	-	-	−0.34 ± 0.11	
KRB	1990–2016	−6.24	−0.24	-	[9]
	1990–2022	−9.44	−0.30		This study
	2003–2021	-	-	−0.42 ± 0.14	
Tailan River Basin	1972–2011	−50.06	−0.29	-	[42]

Table 8. Statistics on other area glacier changes in previous studies.

Region	Period	Area Variation Percentage (%)	APAC (%·a^{-1})	Elevation Change Rates (m·a^{-1})	Source
Altai	1990–2021	−17.10	−0.55	-	[19]
	1976–2009	-	-	−0.44	[43]
Kunlun Mountain Pass	1976–2011	−12	−0.34	-	[44]
West Kunlun Mountain	2013–2019	-	-	0.23 ± 0.06	[45]
Manas River Basin	2000–2020	-	-	−0.18 ± 0.10	[46]
Qilian Mountains	1960–2015	−20.55	−0.37	-	[47]

4.3. Glacier Change Linked to Climate Change

Glacier Changes are mainly controlled by precipitation and temperature [48]. Mann-Kendall (M-K) test, Morlet Wavelet analysis of annual precipitation and average annual accumulated temperature for 1957–2022 at Ahqi meteorological station were done. The results (Figure 10) show that precipitation and accumulated temperature in 1957–2022 showed an increasing trend, the mutation points were 2000 and 1993. The increasing trend in precipitation being more prominent in the last 60 years. The result of Morlet Wavelet analysis showed that precipitation and accumulated temperature changes in the process of the existence of about 2-8a stable cyclic changes, and the main cycle is both 2 years.

This paper uses reanalysis data to investigate the characteristics of climate change in the ARB, aiming to provide a better understanding of the glacier's reaction to climate change. As shown in Figure 11, precipitation, accumulated temperature, cold season precipitation, and ablation-phase accumulated temperature in the ARB showed fluctuating and increasing trends from 1990 to 2022. Cold season precipitation increases significantly in the northeastern of the basin, with greater glacial recharge. The rate of warming was highest in the southeastern basin, and glaciers warmed more rapidly at lower elevations than at higher elevations.

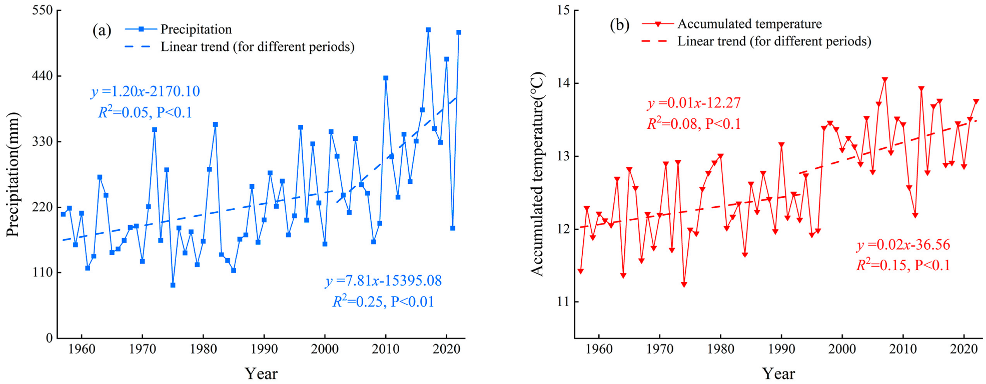

Figure 10. (**a**) Average annual precipitation and (**b**) annual accumulated temperature variation for 1957–2022 at the Ahqi meteorological station.

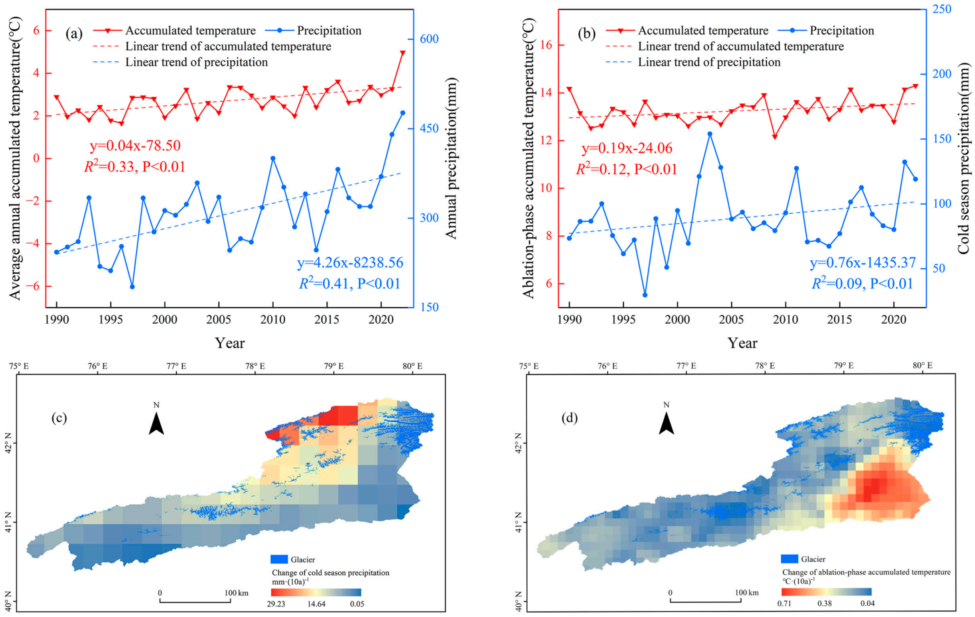

Figure 11. Changes of precipitation and accumulated temperature. (**a**) Annual precipitation and average annual accumulated temperature. (**b**) Cold season precipitation and ablation-phase accumulated temperature in the ARB. Spatial variation of (**c**) cold season precipitation, and (**d**) ablation-phase accumulated temperature in the ARB.

The temperature and precipitation together controlling glacier changes [49]. We explore the glacier variation to climate change by calculating the glacier mass balance sensitivities to driving factors (precipitation, accumulated temperature, cold season precipitation, and ablation-phase accumulated temperature) in the ARB from 2003 to 2021 (Table 9). The results showed that the mass balance sensitivities to precipitation and accumulated temperature are -0.32 ± 0.10 m w.e.a^{-1}(10%)$^{-1}$ and -0.27 ± 0.09 m w.e.a^{-1} °C^{-1}. However, the role of precipitation on glacier accumulation cannot be captured due to the negative mass balance sensitivities to precipitation. Therefore, we calculate mass balance sensitivities to cold season precipitation and ablation-phase accumulated temperature are $+0.27 \pm 0.08$ m w.e.a^{-1}(10%)$^{-1}$ and -0.33 ± 0.10 m w.e.a^{-1} °C^{-1}. The findings indicate that a rise of 1 °C in ablation-phase accumulated temperature cannot be offset by a 10% rise in cold season precipitation. Although the increase rate of cold season precipitation is much greater than the increase rate of ablation-phase accumulated temperature, the glaciers in the ARB are still in an ablation state. Therefore, it is clear that warmer ablation-phase accumulated temperature in the ARB is the main cause of glacier melting.

Table 9. Glacier mass balance and volume sensitivities to driving factors in the ARB.

Sensitivity to Driving Factors	Accumulated Temperature (°C)	Precipitation (mm)	Ablation-Phase Accumulated Temperature (°C)	Cold Season Precipitation (mm)
Mass balance (m w.e.a^{-1})	-0.27 ± 0.09	-0.32 ± 0.10	-0.33 ± 0.10	$+0.27 \pm 0.08$
Volume (10^6 m^3 w.e. a^{-1})	-1453.94 ± 0.82	-1708.38 ± 0.96	-1767.28 ± 0.99	$+1453.94 \pm 0.81$

The mass balance sensitivity to cold season precipitation is $+0.27 \pm 0.08$ m w.e.a^{-1}(10%)$^{-1}$, surpassing the sensitivity of the Altai, Tien Shan, and Pamir to precipitation [50]. Altai and Pamir are located in the north and southwest of ARB, respectively, and ARB is located in the West Tien Shan. The sensitivities of mass balance to ablation-phase accumulated temperature are slightly lower than the Tien Shan sensitivity of -0.42 m w.e.a^{-1}°C^{-1} [50]. Zhang [9] showed that the main cause of glacier retreat in the ARB from 1975 to 2016 was warming temperatures, which aligns with the findings of this study. Previous research has shown that the Altai [19], Nyainqêntanglha Range [51,52], the Qilian Mountain [53], the Ânyêmaqên Mountains [54], as well as the inner Tibetan Plateau in the Geladandong Mountain [55] where glaciers are in a state of melting, and warming temperatures are the main cause of mass loss. Except for the Altai, all other glaciated areas are located in the southern of the ARB. Glacier change is affected by a variety of factors, including climatic factors, especially temperature, which tend to influence glacier change on a large spatial and temporal scale. However, the local environment (elevation and orientations) and the glacier's characteristics (glacier type, size, moraines, and slope) are also glacier changes that can't be ignored as influencing factors [56]. Therefore, it is necessary to consider the multi-influence elements, and in-depth analysis of future climate change on the impact of glaciers, for the ARB integrated water resources management to provide reference.

4.4. Glacier Meltwater and Its Proportion in River Runoff

The presence of snow cover and glaciers has a significant impact on hydrology across a large portion of the Northern Hemisphere [57]. It is important to clarify the role of glacier meltwater in river runoff. Water managers need to understand the impact of glacier ablation and the possible disappearance of water supplies under global climate warming conditions to ensure water security in downstream oases [58]. Wang [43] proposed that glacier meltwater can be accurately estimated by considering the combination of net mass loss and total mass gain; the annual precipitation is the total mass gain of a year. Based on the GPCC, the average annual precipitation for 2003–2009 and 2010–2020 was calculated to be 360.41 mm and 383.79 mm, respectively. Additionally, the estimation for glacier runoff at 11.56×10^8 m^3 w.e.a^{-1} and $11.92.49 \times 10^8$ m^3 w.e.a^{-1}. According to Table 10, the contribution of glacier meltwater to ablation-phase runoff for 2003–2009 and 2010–2020 was 34.57% and 41.56%, respectively. Due to the difference in research methods and time period, our estimates of the glacier meltwater contribution are a little different from the results of previous studies, but generally similar. Compared with 2003–2009, glacier meltwater increased by 7.77% in 2010–2020. The accompanying reduction in glaciers affects the stability of runoff. A few individuals can still survive at high elevations for an extended period, but the amount of meltwater generated will be minimal, and the ability to regulate the runoff will be weakened.

Table 10. Statistics on glacier meltwater and its proportion in previous studies.

Period	River	Proportion in River Runoff (%)	Reference
1991–2000 2000–2008	Aksu-Tarim River	31.40 37.02	[59]
2003–2009 2010–2020	Aksu River	34.57 41.56	This study
1970–2007	Toxkan River Kumalak River	23.00 43.80	[60]
1950s–2005	Toxkan River Kumalak River	24.7 52.4	[61]

5. Conclusions

Using remote sensing images and altimetry data, we extracted the glacier boundary and elevation change in the ARB, analyzed the spatiotemporal changes of the glacier, investigated its reaction to shifts in climate patterns, and clarified the contribution of glacier meltwater to runoff. The ARB glacier area retreated 309.40 km^2 (9.37%, 0.29%·a^{-1}) from 1990 to 2022. Glacier areas at 3000–5000 m have the greatest losses. Glaciers in all directions show a decreasing trend, with the greatest rate of retreat observed in the southeastern. The glacier retreat is transferred from the north to the southeast during 1990–2022. The ARB glacier elevation will generally be thinning from 2003 to 2021. The retreat rate of glacier surface elevation in 2003–2009 and 2010–2021 are 0.35 $\pm$ 0.11 m·a^{-1} (0.30 $\pm$ 0.09 m w.e.a^{-1}), 0.41 $\pm$ 0.13 m·a^{-1} (0.35 $\pm$ 0.11 m w.e.a^{-1}), and the glacier mass change was $-$(962.55 $\pm$ 0.57) $\times$ 10^6 m^3 w.e.a^{-1}, $-$(1087.50 $\pm$ 0.68) $\times$ 10^6 m^3 w.e.a^{-1}, respectively. The distribution and change of glaciers in the ARB have obvious regional variability. The TRB and KRB 1990–2022 glacier area decrease were 61.28 km^2 (0.28%·a^{-1}), 248.13 km^2 (0.30%·a^{-1}), and the glacier surface elevation retreat rate from 2003–2021 was 0.34 $\pm$ 0.11 m·a^{-1}, 0.42 $\pm$ 0.14 m·a^{-1}. The KRB glacier retreats faster compared to the TRB. The mass balance sensitivities to cold season precipitation and ablation-phase accumulated temperature are +0.27 $\pm$ 0.08 m w.e.a^{-1}(10%)$^{-1}$ and $-$0.33 $\pm$ 0.10 m w.e.a^{-1}°C^{-1}. Warmer ablation-phase accumulated temperatures dominate glacier retreat in the ARB. Glacier meltwater accounted for 34.57% and 41.56% of the Aksu River's ablation-phase runoff during the 2003–2009 and 2010–2020, respectively. This study explores the glacial changes, provides an important reference for the integrated management of water resources in the ARB, maintains the survival of the poplar forests in the Tarim River and the downstream "green corridor", and ensures the safety of water used for agriculture in the downstream area.

Author Contributions: Conceptualization, P.R. and T.L.; methodology, P.R.; software, P.R.; validation, P.R.; formal analysis, Y.H.; investigation, P.R.; resources, T.L., X.C. and S.A.; data curation, P.R. and X.W.; writing—original draft preparation, P.R.; writing—review and editing, T.L., Y.H. and X.P.; visualization, P.R.; supervision, P.R.; project administration, T.L.; funding acquisition, T.L. and P.C. All authors have read and agreed to the published version of the manuscript.

Funding: This research was funded by the Third Xinjiang Scientific Expedition Program (Grant No. 2021xjkk1400), Key R&D Program of Xinjiang Uygur Autonomous Region (Grant No. 2022B03021-2), Key Program of National Natural Science Foundation of China (42230708), K.C.Wong Education Foundation (Grant No. GJTD-2020-14), the Xinjiang Uygur Autonomous Region Hydrological Bureau (Grant No. XSKJ-2023-10), Xinjiang Uygur Autonomous Region Natural Disaster Comprehensive Monitoring and Early Warning Center (Grant No.2023000146).

Data Availability Statement: Landsat TM/ETM+ images in 1990, 2000, 2010 and the Sentinal-2 images were downloaded from United States Geological Survey (USGS) and European Space Agency (ESA) at http://www.usgs.gov (accessed on 25 April 2024) and https://www.esa.int (accessed on 25 April 2024), respectively. RGI 6.0 data were downloaded from National Snow and Ice Data Center (NSIDC) at https://nsidc.org/data/glacier_inventory/ (accessed on 25 April 2024). SRTM DEM were downloaded from United States Geological Survey (USGS) at https://earthexplorer.usgs.gov/ (accessed on 25 April 2024). ICESat/GLAS 14 and CryoSat-2 products were downloaded from National Snow and Ice Data Center (NSIDC) and European Space Agency (ESA) at https://nsidc.org/data/glah14/versions/34 (accessed on 25 April 2024) and https://eocat.esa.int/ (accessed on 25 April 2024) respectively. Akqi Meteorological Station data were downloaded from National Meteorological Science and Data Center at https://data.cma.cn/ (accessed on 25 April 2024). GPCC and ERA5-Land data were downloaded from Deutscher Wetterdienst and European Center for Medium-Range Weather Forecasts at https://www.dwd.de/EN/ourservices/gpcc/gpcc.html (accessed on 25 April 2024) and https://cds.climate.copernicus.eu (accessed on 25 April 2024) respectively.

Conflicts of Interest: The authors declare no conflicts of interest.

References

1. Chen, Y.; Li, W.; Deng, H.; Fang, G.; Li, Z. Changes in Central Asia's water tower: Past, present and future. *Sci. Rep.* **2016**, *6*, 35458. [CrossRef] [PubMed]
2. Pieczonka, T.; Bolch, T. Region-wide glacier mass budgets and area changes for the Central Tien Shan between ~1975 and 1999 using Hexagon KH-9 imagery. *Glob. Planet. Chang.* **2015**, *128*, 1–13. [CrossRef]
3. Farinotti, D.; Longuevergne, L.; Moholdt, G.; Duethmann, D.; Mölg, T.; Bolch, T.; Vorogushyn, S.; Güntner, A. Substantial glacier mass loss in the Tien Shan over the past 50 years. *Nat. Geosci.* **2015**, *8*, 716–722. [CrossRef]
4. Liu, D. Glaciers in response to recent climate warming in western China. *Quat. Sci.* **2006**, *26*, 762r771.
5. Shi, Y.; Shen, Y.; Kang, E.; Li, D.; Ding, Y.; Zhang, G.; Hu, R. Recent and future climate change in northwest China. *Clim. Chang.* **2007**, *80*, 379–393. [CrossRef]
6. Wortmann, M.; Krysanova, V.; Kundzewicz, Z.; Su, B.; Li, X. Assessing the influence of the Merzbacher Lake outburst floods on discharge using the hydrological model SWIM in the Aksu headwaters, Kyrgyzstan/NW China. *Hydrol. Process.* **2014**, *28*, 6337–6350. [CrossRef]
7. Wang, X.; Chen, R.; Li, H.; Li, K.; Liu, J.; Liu, G. Detection and attribution of trends in flood frequency under climate change in the Qilian Mountains, Northwest China. *J. Hydrol. Reg. Stud.* **2022**, *42*, 101153. [CrossRef]
8. He, Y.; Yang, T.-B.; Ji, Q.; Chen, J.; Zhao, G.; Shao, W.-W. Glacier variation in response to climate change in Chinese Tianshan Mountains from 1989 to 2012. *J. Mt. Sci.* **2015**, *12*, 1189–1202. [CrossRef]
9. Zhang, Q. Glacier Changes in the Tien Shan Region and Their Impact on River Runoff. Ph.D. Thesis, The University of the Chinese Academy of Sciences, Beijing, China, 2021.
10. Pieczonka, T.; Bolch, T.; Junfeng, W.; Shiyin, L. Heterogeneous mass loss of glaciers in the Aksu-Tarim Catchment (Central Tien Shan) revealed by 1976 KH-9 Hexagon and 2009 SPOT-5 stereo imagery. *Remote Sens. Environ.* **2013**, *130*, 233–244. [CrossRef]
11. Brun, F.; Berthier, E.; Wagnon, P.; Kääb, A.; Treichler, D. A spatially resolved estimate of High Mountain Asia glacier mass balances from 2000 to 2016. *Nat. Geosci.* **2017**, *10*, 668–673. [CrossRef]
12. Wang, Q.; Yi, S.; Sun, W. Continuous estimates of glacier mass balance in high mountain Asia based on ICESat-1, 2 and GRACE/GRACE follow-on data. *Geophys. Res. Lett.* **2021**, *48*, e2020GL090954. [CrossRef]
13. Zhang, G.; Bolch, T.; Allen, S.; Linsbauer, A.; Chen, W.; Wang, W. Glacial lake evolution and glacier–lake interactions in the Poiqu River basin, central Himalaya, 1964–2017. *J. Glaciol.* **2019**, *65*, 347–365. [CrossRef]
14. Ouyang, R.; Cheng, W.; Wang, W.; Jiang, Y.; Zhang, Y.; Wang, Y. Research on runoff forecast approaches to the Aksu River basin. *Sci. China Ser. D Earth Sci.* **2007**, *50*, 16–25. [CrossRef]
15. LIU, W.; Wei, W.; Yang, Q.; Tang, X.; Zhang, T. Study on climate change in the Aksu River basin since recent 40 years. *Arid Zone Res.* **2007**, *24*, 339–343. [CrossRef]
16. Fu, L.-X.; Chen, Y.-N.; Li, W.-H.; He, B.; Xu, C.-C. Relation between Climate Change and Runoff Volume in the Headwatersof the Tarim River during the Last 50 Years. *J. Desert Res.* **2010**, *30*, 204–209. [CrossRef]
17. Chen, A.; Li, Z.; He, J. Study of penetration depth for the SRTM C-band DEM in the glacier area over the High Mountain Asia. *J. Glaciol. Geocryol.* **2018**, *40*, 26–37.
18. McMillan, M.; Shepherd, A.; Gourmelen, N.; Dehecq, A.; Leeson, A.; Ridout, A.; Flament, T.; Hogg, A.; Gilbert, L.; Benham, T. Rapid dynamic activation of a marine-based Arctic ice cap. *Geophys. Res. Lett.* **2014**, *41*, 8902–8909. [CrossRef]
19. Wang, X.; Huang, Y.; Liu, T.; Du, W. Impacts of climate change on glacial retreat during 1990–2021 in the Chinese Altay Mountains. *Catena* **2023**, *228*, 107156. [CrossRef]
20. Bolch, T.; Menounos, B.; Wheate, R. Landsat-based inventory of glaciers in western Canada, 1985–2005. *Remote Sens. Environ.* **2010**, *114*, 127–137. [CrossRef]
21. Ji, Q.; Yang, T.B.; Dong, J.; He, Y. Glacier variations in response to climate change in the eastern Nyainqêntanglha Range, Tibetan Plateau from 1999 to 2015. *Arct. Antarct. Alp. Res.* **2018**, *50*, e1435844. [CrossRef]
22. Guo, W.; Liu, S.; Xu, J.; Wu, L.; Shangguan, D.; Yao, X.; Wei, J.; Bao, W.; Yu, P.; Liu, Q.; et al. The second Chinese glacier inventory: Data, methods and results. *J. Glaciol.* **2015**, *61*, 357–372. [CrossRef]
23. Kaldybayev, A.; Chen, Y.; Vilesov, E. Glacier change in the Karatal river basin, Zhetysu (Dzhungar) Alatau, Kazakhstan. *Ann. Glaciol.* **2016**, *57*, 11–19. [CrossRef]

24. Flament, T.; Rémy, F. Dynamic thinning of Antarctic glaciers from along-track repeat radar altimetry. *J. Glaciol.* **2012**, *58*, 830–840. [CrossRef]
25. McMillan, M.; Shepherd, A.; Sundal, A.; Briggs, K.; Muir, A.; Ridout, A.; Hogg, A.; Wingham, D. Increased ice losses from Antarctica detected by CryoSat-2. *Geophys. Res. Lett.* **2014**, *41*, 3899–3905. [CrossRef]
26. Wouters, B.; Martin-Español, A.; Helm, V.; Flament, T.; van Wessem, J.M.; Ligtenberg, S.R.; Van den Broeke, M.R.; Bamber, J.L. Dynamic thinning of glaciers on the Southern Antarctic Peninsula. *Science* **2015**, *348*, 899–903. [CrossRef] [PubMed]
27. Weiming, C.; Nan, W.; Shangmin, Z.; Yue, F.; Min, Z. Growth of the Sayram Lake and retreat of its water-supplying glaciers in the Tianshan Mountains from 1972 to 2011. *J. Arid Land* **2016**, *8*, 13–22. [CrossRef]
28. Zhang, Y.; Pang, Y.; Cui, D.; Ma, Y.; Chen, L. Accuracy Assessment of the ICESat-2/ATL06 Product in the Qilian Mountains Based on CORS and UAV Data. *IEEE J. Sel. Top. Appl. Earth Obs. Remote Sens.* **2020**, *14*, 1558–1571. [CrossRef]
29. Hall, D.K.; Bayr, K.J.; Schöner, W.; Bindschadler, R.A.; Chien, J.Y. Consideration of the errors inherent in mapping historical glacier positions in Austria from the ground and space (1893–2001). *Remote Sens. Environ.* **2003**, *86*, 566–577. [CrossRef]
30. Williams Jr, R.; Hall, D.; Sigurƒsson, O.; Chien, J. Comparison of satellite-derived with ground-based measurements of the fluctuations of the margins of Vatnajökull. *Iceland* **1973**, *1992*, 72–80. [CrossRef]
31. Krysanova, V.; Wortmann, M.; Bolch, T.; Merz, B.; Duethmann, D.; Walter, J.; Huang, S.; Tong, J.; Buda, S.; Kundzewicz, Z.W. Analysis of current trends in climate parameters, river discharge and glaciers in the Aksu River basin (Central Asia). *Hydrol. Sci. J.* **2015**, *60*, 566–590. [CrossRef]
32. Huss, M. Density assumptions for converting geodetic glacier volume change to mass change. *Cryosphere* **2013**, *7*, 877–887. [CrossRef]
33. Aizen, V.B.; Aizen, E.M.; Melack, J.M. Precipitation, melt and runoff in the northern Tien Shan. *J. Hydrol.* **1996**, *186*, 229–251. [CrossRef]
34. Aizen, V.B.; Aizen, E.M.; Dozier, J.; Melack, J.M.; Sexton, D.D.; Nesterov, V.N. Glacial regime of the highest Tien Shan mountain, Pobeda-Khan Tengry massif. *J. Glaciol.* **1997**, *43*, 503–512. [CrossRef]
35. Aizen, V.B.; Kuzmichenok, V.A.; Surazakov, A.B.; Aizen, E.M. Glacier changes in the Tien Shan as determined from topographic and remotely sensed data. *Glob. Planet. Chang.* **2007**, *56*, 328–340. [CrossRef]
36. Wang, P.-Y.; Li, Z.-Q.; Cao, M.; Li, H.-L. Variation of Qingbingtan glacier No. 72 in Mt. Tuomuer region during past 45 years. *Sci. Geogr. Sin./Dili Kexue* **2010**, *30*, 962–967.
37. Luo, Y.; Li, H.; Li, Z. The relationship between the mass balances and meteorological factors at the glacier of No. 72, Qingbingtan, Shenqi Peak, Tuomuer Area. *J. Arid Land Resour. Environ.* **2012**, *26*, 62–67. [CrossRef]
38. Wang, P.; Li, Z.; Li, H.; Wang, W.; Zhou, P.; Wang, L. Characteristics of a partially debris-covered glacier and its response to atmospheric warming in Mt. Tomor, Tien Shan, China. *Glob. Planet. Chang.* **2017**, *159*, 11–24. [CrossRef]
39. Yanjun, C.; Mingjun, Z.; Zhongqin, L.; Shuang, J.; Wenbin, W.; Shengjie, W. Understanding the mass balance characteristics of Qingbingtan Glacier No. 72 during the period of 2008–2014. *J. Glaciol. Geocryol.* **2020**, *42*, 318–331. [CrossRef]
40. Xing, W.; Li, Z.; Zhang, H.; Zhang, M.; Liang, P.; Mu, J. Spatial-temporal variation of glacier resources in Chinese Tianshan Mountains since 1959. *Acta Geogr. Sin.* **2017**, *72*, 1594–1605. [CrossRef]
41. Oerlemans, J. Quantifying global warming from the retreat of glaciers. *Science* **1994**, *264*, 243–245. [CrossRef]
42. Huai, B.; Li, Z.; Sun, M.; Zhou, P. Glaciers change in the Tailan River watershed in the last 40 years. *Sci. Geogr. Sin.* **2014**, *34*, 229–236.
43. Wang, P.; Li, H.; Li, Z.; Yu, F.; He, J.; Dai, Y.; Wang, F.; Chen, P. Cryosphere changes and their impacts on regional water resources in the Chinese Altai Mountains from 2000 to 2021. *Catena* **2024**, *235*, 107644. [CrossRef]
44. Li, C.; Yang, T.; Tian, H. Variation of west Kunlun mountains glacier during 1990–2011. *Prog. Geogr.* **2013**, *32*, 548–559.
45. Tao, L.; Chao, L.; Xiang, S.; Liming, J.; Hansheng, W.; Gang, L.; Hui, L. Monitoring glacier mass balance of the West Kunlun Mountains over the past 20 years by bistatic InSAR and ICESat-2 altimetry measurements. *Acta Geod. Cartogr. Sin.* **2023**, *52*, 917.
46. Yan, L.; Wang, J.; Shao, D. Glacier mass balance in the manas river using ascending and descending pass of sentinel 1a/1b data and srtm dem. *Remote Sens.* **2022**, *14*, 1506. [CrossRef]
47. He, J.; Wang, N.; Chen, A.a.; Yang, X.; Hua, T. Glacier changes in the Qilian Mountains, Northwest China, between the 1960s and 2015. *Water* **2019**, *11*, 623. [CrossRef]
48. Pan, B.; Zhang, G.; Wang, J.; Cao, B.; Geng, H.; Zhang, C.; Ji, Y. Glacier changes from 1966–2009 in the Gongga Mountains, on the south-eastern margin of the Qinghai-Tibetan Plateau and their climatic forcing. *Cryosphere* **2012**, *6*, 1087–1101. [CrossRef]
49. IPCC. *Working Group I Contribution to the IPCC Fifth Assessment Report: Climate Change 2013: The Physical Science Basis, Summary for Policymakers*; IPCC UN: Geneva, Switzerland, 2013.
50. Radić, V.; Hock, R.C. Regionally differentiated contribution of mountain glaciers and ice caps to future sea-level rise. *Nat. Geosci.* **2011**, *4*, 91–94. [CrossRef]
51. Mo, Q.; Liu, S.; Ma, Y.; Li, M. Glacier elevation changes monitoring in Nyainq(e)ntanglha Range using ICESat. *Sci. Surv. Mapp.* **2018**, *43*, 59–65. [CrossRef]
52. Ren, S.; Menenti, M.; Jia, L.; Zhang, J.; Zhang, J.; Li, X. Glacier mass balance in the Nyainqentanglha Mountains between 2000 and 2017 retrieved from ZiYuan-3 stereo images and the SRTM DEM. *Remote Sens.* **2020**, *12*, 864. [CrossRef]
53. Wang, Y.; Ren, J.; Qin, D.; Qin, X. Regional glacier volume changes derived from satellite data: A case study in the Qilian Mountains. *J. Glaciol. Geocryol.* **2013**, *35*, 583–592.

54. Jiang, Z.; Liu, S.; Guo, W.; Li, J.; Long, S.; Wang, X.; Wei, J.; Zhang, Z.; Wu, K. Recent surface elevation changes of three representative glaciers in Ányêmaqên Mountains, source region of Yellow River. *J. Glaciol. Geocryol.* **2018**, *40*, 231–237.
55. Liu, L.; Jiang, L.; Zhang, Z.; Wang, H.; Ding, X. Recent accelerating glacier mass loss of the Geladandong Mountain, Inner Tibetan Plateau, estimated from ZiYuan-3 and TanDEM-X measurements. *Remote Sens.* **2020**, *12*, 472. [CrossRef]
56. Tian, H.-Z.; Yang, T.-B.; Lv, H.; Li, C.-X.; He, Y.-B. Climate change and glacier area variations in China during the past half century. *J. Mt. Sci.* **2016**, *13*, 1345–1357. [CrossRef]
57. Barnett, T.P.; Adam, J.C.; Lettenmaier, D.P. Potential impacts of a warming climate on water availability in snow-dominated regions. *Nature* **2005**, *438*, 303–309. [CrossRef] [PubMed]
58. Koboltschnig, G.; Schöner, W. The relevance of glacier melt in the water cycle of the Alps: The example of Austria. *Hydrol. Earth Syst. Sci.* **2011**, *15*, 2039–2048. [CrossRef]
59. Bolch, T.; Duethmann, D.; Wortmann, M.; Liu, S.; Disse, M. Declining glaciers endanger sustainable development of the oases along the Aksu-Tarim River (Central Asia). *Int. J. Sustain. Dev. World Ecol.* **2022**, *29*, 209–218. [CrossRef]
60. Zhao, Q.; Ye, B.; Ding, Y.; Zhang, S.; Yi, S.; Wang, J.; Shangguan, D.; Zhao, C.; Han, H. Coupling a glacier melt model to the Variable Infiltration Capacity (VIC) model for hydrological modeling in north-western China. *Environ. Earth Sci.* **2013**, *68*, 87–101. [CrossRef]
61. Wang, Q.; Zhang, J.; Fu, Y. Runoff change and its influencing factors under changing environment in Tarim River. *Bull. Soil Water Conserv.* **2010**, *30*, 99–109. [CrossRef]